Faraday Discussions

Accepted Manuscript

This manuscript will be presented and discussed at a forthcoming Faraday Discussion meeting. All delegates can contribute to the discussion which will be included in the final volume.

Register now to attend! Full details of all upcoming meetings: http://rsc.li/fd-upcoming-meetings

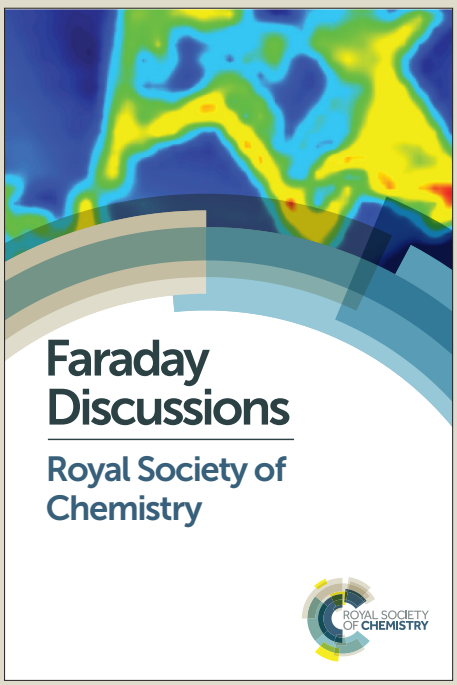

This is an *Accepted Manuscript*, which has been through the Royal Society of Chemistry peer review process and has been accepted for publication.

Accepted Manuscripts are published online shortly after acceptance, before technical editing, formatting and proof reading. Using this free service, authors can make their results available to the community, in citable form, before we publish the edited article. We will replace this *Accepted Manuscript* with the edited and formatted *Advance Article* as soon as it is available.

You can find more information about *Accepted Manuscripts* in the Information for Authors.

Please note that technical editing may introduce minor changes to the text and/or graphics, which may alter content. The journal's standard Terms & Conditions and the Ethical guidelines still apply. In no event shall the Royal Society of Chemistry be held responsible for any errors or omissions in this *Accepted Manuscript* or any consequences arising from the use of any information it contains.

ROYAL SOCIETY OF CHEMISTRY

www.rsc.org/faraday_d

Cite this: DOI: 10.1039/c0xx00000x

www.rsc.org/xxxxxx

ARTICLE TYPE

On a role of liquid intermediates in nucleation of gold sulfide nanoparticles in aqueous media

Maxim Likhatski,*[a] Anton Karacharov,[a] Alexander Kondrasenko and Yuri Mikhlin[a]

Received (in XXX, XXX) XthXXXXXXXXX 20XX, Accepted Xth XXXXXXXXX 20XX

DOI: 10.1039/b000000x

Previously, we found a series of fluid nanoscale intermediates preceding nucleation of gold sulfide in the reaction between aqueous $HAuCl_4$ and sodium sulfide. Here, the effect of temperature, addition of an inert electrolyte and some other factors on characteristics of the "dense liquid" intermediates and the formation of solid nuclei were studied using UV-vis absorption spectroscopy, DLS, zeta-potential measurements, SAXS. It was revealed, in particular, that the negatively charged interfaces of the dense liquid species critically impede their fusion into large enough dense droplets in which nucleation can take place. The nucleation and following coagulation of poorly crystalline gold sulfide proceed not instantly but progressively as the dense liquid droplets arise, with the process being sharply accelerated by the injection of NaCl or temperature increase.

.

Introduction

Recently, we explored the reduction of aqueous gold chloride complexes with sulfide ions yielding gold, gold sulfide nanoparticles or their mixture, depending on the reactant ratio,[1-3] which are of vivid interest for geochemistry and mineral processing of gold, and for preparation of Au_2S nanoparticles and Au_2S-Au hybrid nanomaterials for plasmonics, surface enhanced Raman spectroscopy (SERS), biomedical applications.[4-7] A series of long-lived pre-crystallization intermediates was found to arise in the reaction with the molar ratio $Na_2S/HAuCl_4$ higher than 2 at room temperature.[3] The "soft" droplet-like species from 10-50 nm to about 200 nm and more in the lateral size were directly imaged using *in situ* tapping-mode atomic force microscopy (AFM) (Fig. 1), in good agreement with time-resolved dynamic light scattering (DLS) and small-angle X-ray scattering (SAXS) data. The findings were rationalized in terms of accumulation of reduced $Au_mS_n^-{\cdot}pH_2O$ solutes (referred as pre-nucleation clusters after Gebauer and Cölfen[8]) in dense liquid domains of various dimensions, including "liquid clusters" less than about 20 nm, globules about 50 nm and their submicrometer aggregates. Nucleation was suggested, in accordance with the two step nucleation mechanism,[9-12] to proceed within "dense droplets" large enough to accumulate necessary amount of Au-S substance formed via coalescence of the above fluid species, which probably is a slow stage determining the rate of gold sulfide formation at room temperature. We believe that there are several sorts of dense liquid "droplets" accumulating the pre-nucleation species arise, evolve with time, temperature, etc., and serve as submicrometer "reactors" for nucleation in the case of Au-S system. This results in a very long, up to few days, existence of the liquid intermediates, making possible their detection and characterization before abrupt sedimentation of poorly crystalline gold sulfide occurs. The phenomena are important for understanding both the fundamentals of nucleation and crystal growth in aqueous solutions and the specific chemistry of colloidal gold and gold sulfide in sulfide-containing media. Moreover, there are experimental evidences of an involvement of fluid intermediates in the well-known synthesis of Au NPs by citrate reduction of aqueous tetrachloroaurate,[13,14] formation of PtS and PdS nanoparticles, and some other media with effectively retarded chemical reaction or(and) nucleation stages.

Here, we report the results of a study on the effect of temperature, indifferent electrolyte and some other factors on properties of the fluid intermediates formed in the aqueous $HAuCl_4$– Na_2S system with the molar ratio 1:3. A set of in situ experimental techniques including UV-vis absorption spectroscopy, DLS, zeta-potential measurements and SAXS was applied in an attempt to monitor the changes of dimensions and properties of dense liquid species and to detect the appearance of solid nuclei. The elevation of temperature to 40-70 °C and an addition of NaCl solution at room temperature were employed in order to initiate nucleation of gold sulfide and to relate that with evolution of the transient liquid species.

Experimental

In all the experiments performed deionized Milli-Q Pore water with no additional purification was used. A portion of 10 mM sodium sulfide solution (3 ml) was quickly added to agitated 0.3 temperature, freshly prepared from 0.1 M $HAuCl_4$ stock solution (Krasnoyarsk Plant of Non-Ferrous Metals). The solution was

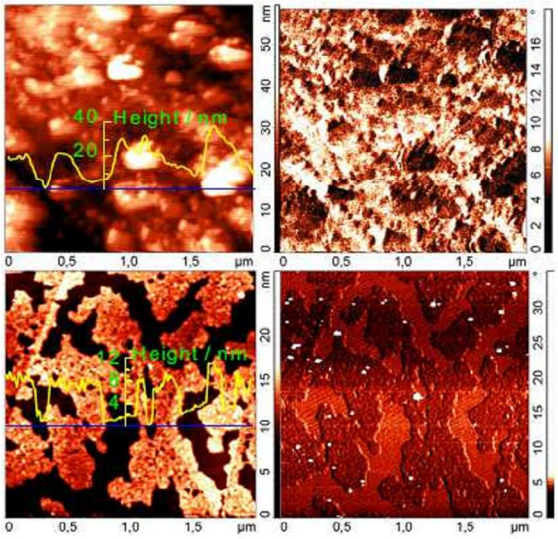

Fig. 1 Tapping-mode AFM height (left panels) and phase images of the products formed with Na2S/HAuCl4 ratio of 3 acquired in situwithin about 2 h after mixing the reagents (upper panels) and ex situof a solution drop dried on HOPG in air (adapted from Ref.3). One can see voluminous species in the solution producing a thin film upon drying.mM $HAuCl_4$ (32.5 ml) on air and thermostated at desired

agitated for one min, then agitation was switched off. All the chemicals were analytical grade and used as received. UV-vis absorption spectra were acquired in the wavelength range 200 nm to 1200 nm using an Evolution300 spectrophotometer (Thermo Scientific) in a thermostated 1 cm quartz cell. Dynamic light scattering studies and zeta-potential measurements were performed with a Zetasizer Nano ZS device (Malvern Instruments) at scattering angle 173°. The intensity weighted mean size is normally used in this study due to its high reliability, although the results of multimodal fitting also were taken into consideration.

SAXS measurements were performed at the Austrian SAXS beamline at the ELETTRA synchrotron, Trieste, Italy.[15] The time-resolved experiments was conducted with an aliquot of the solution immediately after mixing of the reactants loaded in a standard X-ray quartz capillary (inner diameter of 1.5 mm) sealed and temperature-controlled with the Peltier heating/cooling sample holder (Anton Paar). The SAXS data were acquired at photon energy of 8 keV applying 2D Pilatus 100K detector system. The common procedures of radial averaging and normalization were employed to obtain 1D $I(q)$ *vs* q curves, where $q = (4\pi/\lambda)\sin\theta$ is wave vector, $I(q)$ is scattering intensity, λ=0.154 nm is the wavelength used, and 2θ is the scattering angle.

Results

UV-vis spectroscopy

Fig. 2 shows typical UV-vis absorption spectra of yellow-brown reaction media with the initial composition of0.3 mM $HAuCl_4$ + 1 mM Na_2S, which, after a few seconds of reaction, become smooth curves having neither the peak of tetracholoroaurate at 315 nm nor plasmon maxima of gold nanoparticles. The

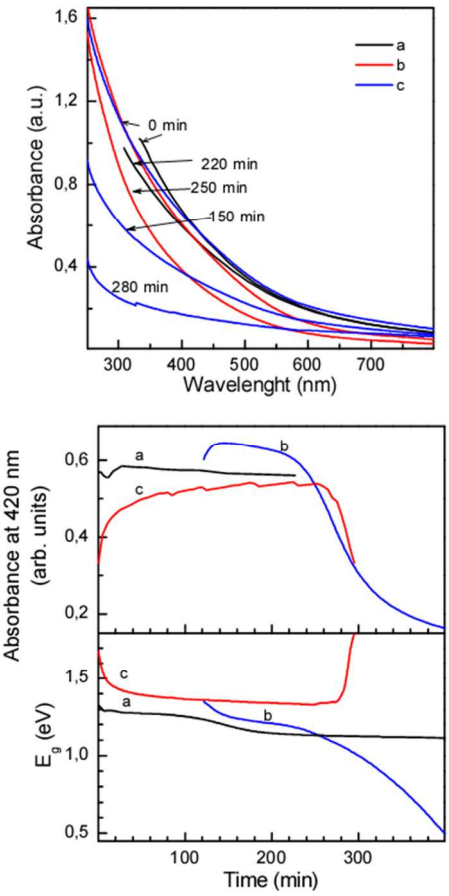

Fig. 2 Typical UV-vis absorption spectra and absorbance at 420 nm and the band gap width vs reaction time for 0.3 mM $HAuCl_4$ + 1 mM Na_2S solution at (a) 21 °C, (b) after addition of 0.05 M NaCl to the solution reacted for 2 h, and (c) at 70 °C.

absorbance magnitudes at a wavelength of 420 nm and the plots of $(\alpha E_{ph})^{1/2}$ vs E_{ph} (α is the absorption coefficient, E_{ph} is the discrete photon energy) were further used to estimate temporal changes in the spectra intensity and shape and in the band gap width E_g of disordered matter produced, assuming an indirect electronic transition. The absorption increases in the starting period (about 30 min) and stays almost constant as long as several days at room temperature. Addition of a strong electrolyte, 5mM sodium chloride, that approximately doubled the ionic strength of this rather stable solution (after 2 h reaction), causes some increase in the optical absorption, which then decreases gradually over about 2 h and more rapidly after that. Except the starting period, the E_g values vary in the same manner.

The absorbance at an elevated temperature (70 °C) grows rapidly in the first minutes and then slowly change still a sharp drop, while the E_g magnitude alters antipathetically. In general, the absorbance at enhanced temperatures is lower and the band gap is wider than at the room temperature. Both in the high temperature and the NaCl addition experiments, formation of a bulky black residue and the solution bleaching related with the optical absorption decay were observed. Moreover, minor amounts of suspended solids could be seen by the naked eye in these systems well before the bulky sedimentation. The findings confirm that the absorbance is due soluble (colloidal) products, whereas the pronounced reduction of the spectrum intensity is

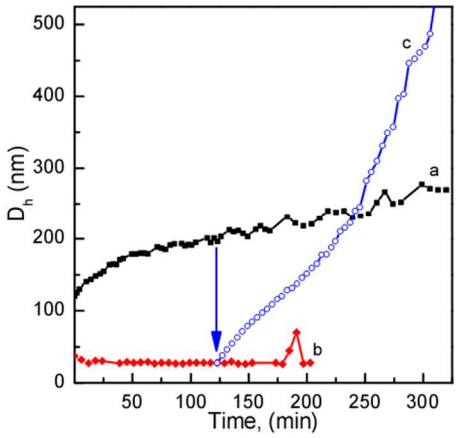

Fig.3 Average hydrodynamic diameter of the species determined using DLS vs reaction time for 0.1 mM $HAuCl_4$ +0.3 mM Na_2S media at (a)21°C, (b) 70 °C and (c) after addition of 0.05 M NaCl to the solution reacted for 2 h at 21 °C.

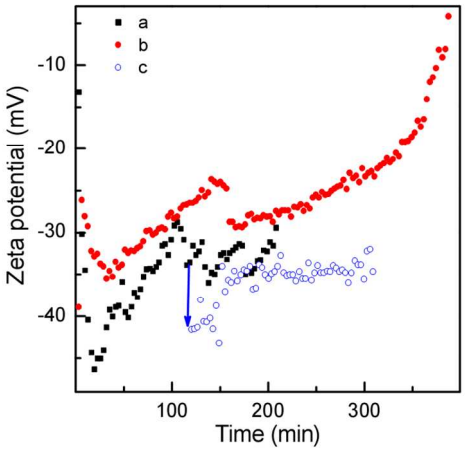

Fig.4 Evolution of zeta-potentials with reaction time of the species formed in0.3 mM $HAuCl_4$ + 1 mM Na_2Ssolution at (a)21 °C, (b) 65 °C and (c) after addition of 0.05 M NaCl to the solution reacted for 2 h at 21 °C

caused by coagulation of solid particles, which were found to be composed of poorly crystalline cuprite-type Au_2S somewhat enriched with sulfur but easily decomposed to sulfur-capped metal gold nanoparticles.[1,2,3] The value referred as the indirect band gap E_g that varies in the range 1.7 eV to 1.2 eV is thought to be determined by Au(I)-S bonding, decreasing with shortening the bond length as the nanometer liquid clusters coalescence into larger droplets and the matter within the droplets becomes denser and more ordered (see below). The steep E_g decline in the media with additional NaCl may be due to Au-Cl bonding in the solution with low residual concentration of sulfide ions. It should be mentioned that the process rates, especially at the elevated temperatures, notably depend on agitation, air access and other factors. In some cases, instability regions several min long were observed after sharp initial changes of the absorbance and E_g and just before the bulky precipitation at 60-70 °C.

Dynamic light scattering

Fig. 3 shows average hydrodynamic size (D_h) of scattering particles as a function of time at two temperatures and after the addition of sodium chloride. At room temperature, the scatterers grow to several hundred nm over several hours, in concord with dimensions of "soft" droplet-like entities directly observed in the solution using *in situ* AFM.[3] The addition of NaCl solution after 2 h reaction results in a seeming decrease of the particles and then their rapid growth up to a micrometer and bigger. Interestingly, the mean hydrodynamic size of the particles usually increases more slowly at 70 °C. The DLS data suggest polydisperse composition of the systems under many conditions, particularly, in the initial stages and before the precipitation. Multimodal fit of the correlation functions (the quantitative results are not quite reliable and are not shown in Figures) shows that the main volume contribution is provided by particles as small as 10-20 nm at room temperature[3] and 3-10 nm at 70 °C in the conditional stability regions, although their scattering intensity is minor. The situation in case of NaCl added is even more complicated as the volumes of different size scatterers are often comparable.

Zeta-potential

Zeta-potentials measured in the systems (Fig. 3) are always negative, with the magnitude increasing from -10 mV to -40±5 mV in the initial stage when rather fast growth of the species was observed. The potential values stay nearly constant in the quasi-stationary regions, and the one approaches zero as gold sulfide residue precipitates. One can conclude from the comparison of the data on zeta-potential and the hydrodynamic diameter time variation that the entities are stabilized, first of all, due to the electrically charged interfaces, with the negative charge seems to be produced by both hydrosulfide anions and chloride-ions. The

injection of additional sodium chloride initially causes an increase in the negative zeta-potential of the species (Fig. 3, c). In the next stage, zeta potential reduces owing to higher electrolyte concentration, promoting further aggregation. Noteworthy, the study of zeta-potential time evolution was complicated by an impact of the imposed electric field on properties of hydrosols. To minimize side effects, the experiments were also conducted using fresh portions of the solution sampled at pre-determined time intervals; principally the same results were obtained.

SAXS

In contrast to DLS, SAXS patterns acquired at the wave vector q above 0.1 nm^{-1} are sensitive to nanoparticles smaller than 20-30 nm, allowing to monitor their evolution and, in principle, to detect the formation of solid nuclei. The polydispersity of the scatterer size was taken into account by using the Schultz-Zimm statistical distribution of the scatterer core radii. As demonstrated above, the particles tend to form aggregates. Hence, a model taking into account some stickiness of the scatterers should be applied. For simplicity, the hard sphere potential combined with rectangular well attractive potential[16] was considered to model the inter-particles interaction in decoupling approximation.[17] In the simplest case, the intensity of the scattered radiation is given by

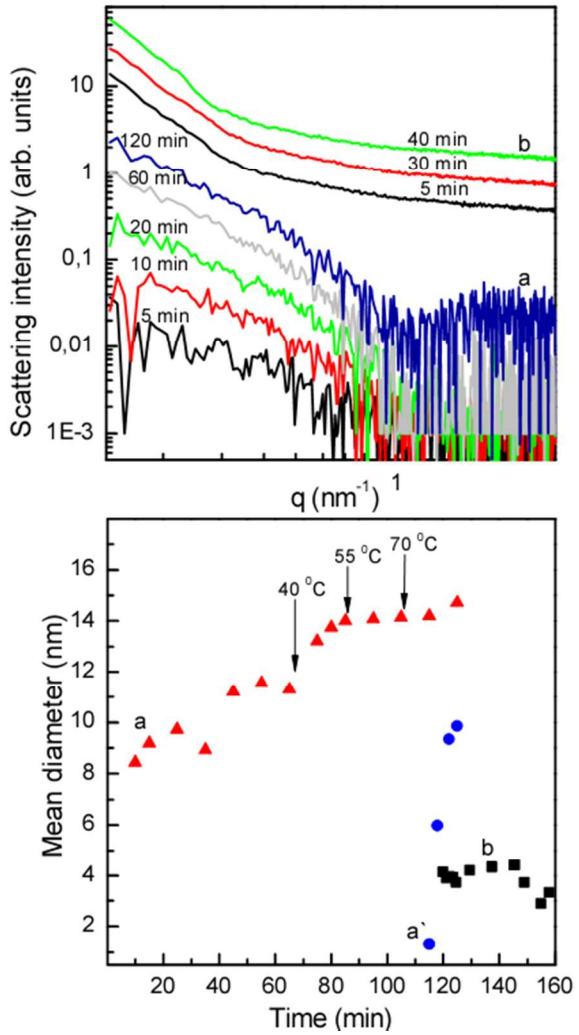

Fig. 5. SAXS curves acquired from a capillary filled with 0.3 mM $HAuCl_4$ + 1 mM Na_2S solutionwith programmable temperature changes (a), and that from a capillary containingthe solution reacted for 2 hours under room temperature + 0.05M NaCl (b) along with time dependenceof the mean diameters of the species.

$$I(q) = scale \cdot \langle F^2(q) \rangle_R \cdot S(q, R_{HS}, \lambda, \varepsilon, \varphi) + c_p \cdot q^{-n} + bkg$$

Here q is the value of the scattering vector,

$$F(q) = (\rho_{scatterer} - \rho_{media}) \cdot V \cdot f(qR))$$

is the form factor amplitude of a scatterer having electron density $\rho_{scatterer}$, and ρ_{media} is the electron density of the media where the scatterers exist; $f(qR) = (3 \sin qR - qR \cos qR)/q^3R^3$ is the form factor of a sphere with radius R, and V is the volume of a sphere of that radius. $\langle F^2(q) \rangle_R$ stands for averaging over scattering potentials of the scatterers of different radii R, with Schultz distribution being the weighting function. The averaging was performed by a numerical integration. $S(q, R_{HS}, \lambda, \varepsilon, \varphi)$ is the structure factor based on the sticky hard-sphere inter-scatterer interaction potential model.[16] Here, R_{HS} is the radius of the hard sphere, φ is the apparent volume fraction of the scatterers in the solution, with λ-1 and ε representing the range and strength of the attraction. The radius of a scatterer R was assumed to be equal to that of the hard sphere. Because of the agglomeration of scatterers takes place, we have added a generalized power law term $c_p \cdot q^{-n}$ to the fitting function. When it was required, the second fraction of the sticky hard-sphere scatterers was considered.

SAXS curves acquired at temperature changing in a programmable manner are shown in Fig. 5 (top). The arrows shown on the plot of the mean diameter *vs* time (bottom) mark the start of temperature elevations, with the rate of heating being 20 ºC/min. In 5 min after the start of the reaction at room temperature, the scattering curves can be fitted using a single fraction of sticky hard spheres with diameter ~8.5 nm, and some growth was observed with time. The main transformations of the SAXS curves occur within about 1 h after the start of the reaction, with results of the fits showing the species growth from 8.5 nm to 13 nm. After 110 min of the reaction and the temperature of 70 °C reached, the single fraction model function fits the experimental data unsatisfactorily, and, therefore, the second fraction of sticky hard spheres should be added to the model functions for $I(q)$. The initial mean diameter of the second fraction scatterers is of 1.32±0.4 nm and quite rapidly increases with time. This can be rationalized in terms of nucleation and growth of solid nanoparticles, but not liquid species observed before this point. Then, rapid aggregation of solid nanoparticles results in partly suspended black bulk residue.

Almost immediately as 0.05 M NaCl solution was added to the system reacted at ambient temperature for 2 hour, comparatively tiny species of ~4 nm attributable to solid nanoparticles were revealed together with the ~15 nm species (liquid clusters) (Fig. 5, curves b). The volume of the nanoparticles estimated from the $I(0)$ magnitude continuously decreased with time, probably, due to their aggregation and sedimentation.

Discussion

The experimental data obtained in this and previous work[1,3] demonstrate that the reduction of tetrachloroaurate by excessive sodium sulfide in the concentrations well above the stability range of sulfide and chloride complexes of Au(I) produces fluid droplet-like entities whereas solid particles form in quantities below the detection limit of DLS, SAXS and other techniques. In addition, ^{1}H NMR DOSY technique was applied in attempt to specify water molecules related to the dense droplets. It was found that the average diffusion coefficient is slower about 10% in the media containing dense liquid intermediates. However, the analysis is not straightforward since a considerable contribution of bulk water and pH changes so we avoid to present quantitative data here. It was previously established using in situ and ex situ X-ray absorption spectroscopy, XPS, TEM[2,3] that the supersaturated solutions and precipitated material composed of Au(I) coordinated in average to less than two S atoms. In all the cases, the precipitates characterized here with TEM and XPS were found to be almost identical to poorly crystalline Au(I) sulfide easily decomposing to Au clusters as described in refs. 2, 3.

The initial "liquid clusters" several nm in size have a low negative electrical charge and easily amalgam into larger species up to 20-50 nm in diameter, which exhibit zeta-potentials around

-40 mV impeding their further coalescence. The amount of Au-S substance in the interior is thought to be insufficient for the formation of large enough, stable "critical" nuclei requiring "liquid droplets", which are dense both in terms of absence of internal boundaries and the enhanced concentration and chemical state of the solute. Although the 20-50 nm liquid droplets, or globules, associate into submicrometer aggregates, those are probably loose and have inner interfaces preventing mass transfer and then nucleation. The fusion of liquid intermediates and following nucleation, growth and coagulation of solid particles is expected to be faster in solutions with high background electrolyte concentration due to weaker electrostatic repulsion.

Indeed, the addition of a strong electrolyte triggers the formation and precipitation of gold sulfide. Furthermore, a change of osmotic pressure as inert electrolyte is added can play a role of a "water pump" which renders the substance inside liquid droplets denser. During the growth of the liquid intermediates evidenced with DLS, slow changes of the amount and the chemical state of the pre-nucleation substance were observed from the UV-vis spectra. At certain point, both the size and optical absorption changes notably accelerate, suggesting transformation of the pre-nucleation matter. Simultaneously, SAXS fitting shows the emergence of 1.5-8 nm nanoparticles composed, most likely, of gold sulfide, followed by coagulation of black precipitate. It is important that these phenomena proceed gradually but not instantaneously; this may be explained by a

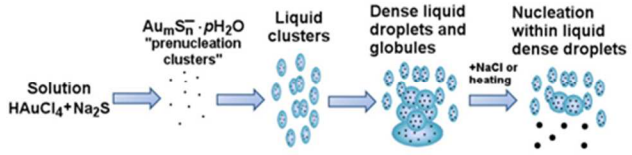

Scheme exhibiting different stages in solution preceding bulk black residue deposition during the reaction studied

progressive transformation of the loose aggregates into the dense droplets and subsequent nucleation in the interior.

This mechanism is illustrated in Scheme showing the evolution of the fluid pre-nucleation entities as in Ref.3 with amendment of the nucleation stage, which is believed to proceed within the large dense droplets, whereas smaller (or loose) fluid species still remain in the solution.

The UV-vis absorption intensities are lower and E_g magnitudes derived from the optical spectra are larger at enhanced temperatures than those at the room temperatures (Fig. 3), suggesting a slower formation of the pre-nucleation substance and "liquid clusters". At the same time, the experimental results imply that the lifetime of large fluid aggregates is shorter. We hypothesize that the emergence of small liquid clusters is hindered, while their fusion into large dense droplets, and then the nucleation stage, is facilitated, probably, because of more diffuse boundaries between the bulk solution and the dense liquid species.

The structures and mechanisms found for the Au-S media may be applicable for other reactions in which nucleation or(and) chemical reaction stages are effectively arrested. In particular, similar results suggesting the existence of long-lived quasi-liquid intermediates, though with some kinetic differences, were obtained in case of the reaction between H_2PtCl_6 and sodium sulfide; these data will be reported in detail elsewhere.

Conclusions

In situ time-resolved UV-vis spectroscopy, DLS, zeta-potential measurements, and synchrotron based SAXS were used in order to study pre-nucleation long-lived fluid species in the reaction of tetrachloroauric acid and sodium sulfide with the initial molar ratio of 1 to 3 at two temperatures. The initial "liquid clusters" were found to have a small negative charge and coalescence into larger species exhibiting negative zeta-potential of about 30-40 mV and associating to submicrometer aggregates. Addition of 0.05 M NaCl sharply accelerates the aggregation and nucleation. The growth of the dense liquid species proceeds slowly at elevated temperatures, although in general the formation of solid gold sulfide is faster, probably, due to easier fusion of the species into large droplets and fast nucleation.

Acknowledgments

This study was supported by the Grant MK-6489.2014.5 for young candidates of science from President of RF. We gratefully thank Prof. Heinz Amenitsch and the staff of the Austrian SAXS beamline at the ELETTRA for their precious assistance.

Notes and references

[a]*Institute of Chemistry and Chemical Technology of the Siberian Branch of the Russian Academy of Sciences, Akademgorodok, 50/24, Krasnoyarsk, 660036, Russia; E-mail: lixmax@icct.ru*

† Electronic Supplementary Information (ESI) available: additional data on SAXS experiments. See DOI: 10.1039/b000000x/

1 Y.Mikhlin,M.Likhatski,A.Karacharov,V. Zaikovski and A. Krylov,*Phys. Chem. Chem. Phys.*,2009,**11**, 5445-5454.
2 Yu. Mikhlin, M. Likhatski, Ye. Tomashevich, A. Romanchenko, S. Erenburg and S.Trubina,*J. Electron Spectrosc.*,2010,**177**, 24-29.
3 Yu.Mikhlin, A. Karacharov, M. Likhatski, T. Podlipskaya, I. Zizak, *Phys. Chem. Chem. Phys.*, 2014,**16**, 4538 – 4543.
4 R.D. Averitt, D. Sarkar and N.J. Halas, *Phys. Rev. Lett.*,1997,**78**,4217-4220.
5 A. M. Schwartzberg, C. D. Grant, T. van Buuren and J. Z.Zhang, *J. Phys. Chem. C*,2007,**111**, 8892-8901.
6 J. Majimel, D. Bacinello, E. Durand, F. Vallée and M. Tréguer-Delapierre, *Langmuir*, 2008,**24**, 4289-4294.
7 A. M. Gobin, E. M. Watkins, E. Quevedo, V. L. Colvin and J. L. West, *Small*,2010,**6**,745-752.
8 D. Gebauer and H. Cölfen,*Nano Today*,2011, **6**, 564-584.
9 P.R. ten Wolde and D. Frenkel,*Science*,1997, **277**, 1975-1978.
10 A. Lomakin, N. Asherie and G. B. Benedek, *Proc. Natl. Acad. Sci. USA*, 2003, **100**, 10254-10257.
11 D. Kashchiev,P. G. Vekilov and A.B. Kolomeisky,*J. Chem. Phys.*,2005, **122**, 244706.
12 P.G. Vekilov, *Nanoscale*, 2010, **2**, 2346-2357.
13 Y. Mikhlin, A.Karacharov, M. Likhatski, T. Podlipskaya, Y. Zubavichus, A. Veligzhanin and V. Zaikovski,*J. Colloid Interf. Sci.*,2011,**362**, 330-336.

14 M. Doyen, K. Bartik and G. Bruylants, *J. Colloid Interf. Sci*.,2013,**399**, 1.
15 S. Bernstorff, H. Amenitsch and P. Laggner, *J. Synchrotron Radiat*., 1998, **5**, 1215–1221.
16 D. Pontoni, S. Finet, T. Narayanan, A.R. Rennie, *J. Chem. Phys.*, 2003, **119**, 6157-6165.
17 J.S. Pedersen, *Adv. Colloid Interf. Sci.*,1997, **70**, 171-210.